Lungs Segmentation by Developing Binary Mask

By

Saleem Iqbal

2006-NUST-MS-PHD-CSE(E)-32

Submitted to the Department of Computer Engineering

in Partial Fulfillment of the Requirements for

MS in Computer Software Engineering

Supervised by

Dr. Amir Hanif Dar

Department of Computer Engineering, College of E&ME

National University of Science and Technology

2009

Thesis Guidance and Evaluation Committee

Dr. Amir Hanif Dar (Supervisor)

Lt Col. Dr. Farooque Azam

Dr. Saad Rehman

Mr. Yasir Jan

Acknowledgements

First of all, I thank GOD for helping me complete the work. I would like to express my gratitude to Dr. Aamir Hanif Dar for his valuable guidance and academic support. I am grateful to Dr. Muhammad Fahim and Dr. Adnan Siddique of Nuclear Medicine, Oncology and Radiotherapy Institute (NORI), Islamabad for providing images and sharing domain knowledge. Mr. Abdul Sattar, Manager Islamabad Diagnostic Centre, Islamabad and Mr. Saeed Ullah Khan Marwat, chief technologist, department of Radiography, Pakistan Institute of Medical Sciences (PIMS), Islamabad deserve my special thanks for providing CT scan images. I would like to thank Mr. Nouman Azam for providing me some good suggestion. Computer Engineering Department also deserves acknowledgment for creating working environment enabling me to accomplish this research work.

Saleem Iqbal

Dedication

Dedicated to
Higher Education Commission
for providing financial support.

Abstract

CT scans have proved to be an important modality for diagnoses of thoracic diseases such as TB, emphysema and cancer. However, soft tissues and minor pathologies are not clearly identifiable from CT. Computer aided processing of CT data can solve the problem. For computer aided diagnoses of lungs diseases, lungs segmentation is a prerequisite. Moreover, lungs segmentation has its application in visualization, volumetric measurement, shape representation and analysis, image guided surgery and nodule size measurement etc. Most of the lungs segmentation methods are scanner dependent. We proposed and implemented a novel, 3-D fully automated machine independent method for segmenting lungs region from CT slices using hybrid approach. Thresholding, mathematical morphology and pixel connectivity have been utilized to achieve the objective. We approached the problem by generating binary mask which identifies the lungs regions on each CT slice. Then, lungs are segmented using the binary mask. The method of generating mask comprised of five steps. 1) Gray level threshold value has been calculated by iterative method and Otsu's method. Results of both methods are same with difference in decimal places only. Iterative method maximizes within class similarity and Otsu's method maximizes between class variance. Using calculated threshold, thresholded binary image has been generated. 2) All objects are identified on the thresholded image by taking advantage of connectivity of pixels and objects connected with border of the image have been removed. These objects were due to attenuation of X-rays through air around the patient. 3) Gaps on region of interest have been stuffed by morphological filling. 4) Trachea, bronchi's and other areas which could be mistaken for lungs have been removed by exploiting anatomical properties of the lungs. 5) Mask boundaries have been smoothed by morphological closing. Finally, lungs have been segmented by arrays product of final mask generated in first step to fifth step and original CT image. The proposed method has been applied on data set of three complete CT scans (20 slices each) and 25 more slices thus in all on 85 slices taken from two different sources. Results have been compared with manually delineated lungs on CT images by a radiologist. Mean Overlapping Fraction, mean precision, mean Sensitivity/Recall, mean Specificity, mean Accuracy and mean F-measure have been calculated and recorded as 0.9900, 0.9962, 0.9966, 0.9977, 0.9992 and 0.9964 respectively.

Table of Contents

List of Figures

List of Tables

List of Abbreviations

CT	Computer Tomography
FN	False Negative
FP	False Positive
LOG	Laplacian of Gaussian
OF	Overlapping Fraction
TN	True Negative
TP	True Positive

Chapter 1

Introduction

1.1 Introduction

This chapter presents an overview of the lungs segmentation from CT slices by developing binary mask, objective of the thesis, applications of segmented lungs including visualization, volumetric measurement, image guided surgery, shape representation, change measurement and lung cancer detection, problems in lungs segmentation, background of the lungs segmentation, proposed method for segmenting lungs. At the end organization of the thesis has been described.

1.2 Overview

Lungs are constituted by masses of alveoli and are protected by the chest box. Alveoli are the tiny sacs at the ends of Bronchioles. Bronchioles are smaller airways spreading from Bronchi. Bronchi are the major airways. Main function of the lungs is exchange of Oxygen and Carbon Dioxide. Lungs are tender part of the body and target of many deadly diseases such as pneumonia, cancer and tuber closes.

Medical imaging has been proved to be very helpful in diagnosis and treatment of lungs diseases for the last century. Specially, Computer Tomography (CT) is the state of the art technique for lungs imaging. It provides high resolution and high contrast images from which different structure and anatomies such as parenchyma, airways, diaphragm, vessels and trachea can be observed. Different pathologies can be diagnosed as well.

Computed Tomography [1] [2] is a well known source of taking images of internal structures of the human body. It consists of an X-ray source and a detector placed on opposite side, patient being lying in between X-ray source and X-ray detector. The machine is set in such a way that the X-ray beam is rotated about an axis while the patient is moved along that axis. In this way, X-ray images of each section are digitally taken from many different angles. Subsequently, tomography an algorithms derived by a mathematical procedure, is applied to reconstruct a three-dimensional matrix of the values. The matrix represents the X-ray transmission properties in the volume occupied by the chest.

Chest CT not only shows lungs but also other anatomical structures as well as pathological structures. The objective is to segment only lungs from CT slices so that diagnose could be made more easily and accurately by the human observers or diagnostic machines. For all computerized analysis and diagnoses, 'Lungs Segmentation' is a pre-requisite.

Lungs Segmentation is the process of distributing pixels in the chest CT image into lungs and non-lungs classes. The lungs recognized in this way have a wide variety of applications in medical diagnosis, research and visualization. Segmentation [3] [4] [5] [6] [7] can also be done for brain, heart, knee, jaw, spine, pelvis, liver, prostate and the blood vessels.

The dataset consists of digital CT slices of chest CT taken at 'Lung Window'. These slices are axial images of the entire thorax. The input to the segmentation procedure is grayscale digital CT image. The output of the method is the segmented lungs from other anatomical structures in the thorax. All anatomical and pathological structures lying on parenchyma remains as it is on the lungs.

The system has been tested on CT images taken from NORI, Islamabad and Islamabad Diagnostic Centre, Islamabad.

1.3 Objectives

One of the most important problem in computer aided lungs diagnosis is segmentation of the lungs as it is a pre-condition in all digital diagnostic systems and very helpful to human observer. The thesis presents a method for automated lungs segmentation. Following are the objectives:

- Accurate segmentation of the left lung and the right lung from CT slices of chest CT scan at lungs window.

- Advancement towards computer aided diagnosis specially lungs cancer nodule detection and size measurement from chest CT scan

- Advancement towards making CT scan more effective for diagnoses of various pulmonary diseases.

1.4 Applications

Image segmentation is the crucial first step when thorough and quantitative information about the appearance, size, or shape of the lungs anatomy is desired. Main applications depending on image segmentation include three-dimensional visualization, volumetric measurement, shape representation of the lungs, image-guided surgery, detection of anatomical changes overtime, lungs cancer detection and nodule size measurement.

1.4.1 Visualization

Segmentation of lungs permits creation of three dimensional surfaces for visualization of the anatomy of the lungs of a patient. The benefit of the surface model representation of lungs is that it provides a three dimensional view of the lungs from any angle, which is an improvement over two-dimensional cross sections through the original grayscale data. Surface models can be generated from segmented lungs using different algorithm. Although three dimensional models could be created directly from grayscale data of the lungs, the segmentation step is used to give the clear picture.

1.4.2 Volumetric Measurement

Measuring volumes of lungs is necessary in some medical studies, both of normal lungs and of various pathological conditions or disorders. This is a clear application of segmentation, since it is not possible to accurately measure lungs volumes visually. For example, in studies of schizophrenia, volume measurement is used for quantifying the variation in neural anatomy. Areas of concern in these studies include the lateral ventricles, structures in the temporal lobe such as the hippocampus, amygdale, and parahippocampal gyros, the plenum temporal, and the corpus callosum. It is a time taking process to obtain accurate measurements of such regions. Similar diagnoses could be made for lungs

1.4.3 Shape Representation and Analysis

Many quantitative representations of shape are studied for mathematically describing salient anatomical characteristics of the lungs. The first step in creating a representation of anatomical shape of the lungs is segmentation. Intuitively, the lungs' position and location of its boundaries are needed for studying lungs.

Most probably, shape representations will become increasingly useful in making quantitative anatomical comparisons of the lungs. Distance transforms shape representations have already been applied to the classification of anatomical structures in different studies that aim to differentiate between the hippocampus-amygdale complexes of schizophrenics and normal.

Shape representations can also be used to help the segmentation process itself by providing anatomical knowledge. A generative shape model, trained from a population of shape representations, can then be used to imagine new shapes according to the learned modes of variance in the shape population. This allows visualization of "average" anatomy and of the main anatomical variations that could happen. Finally, at each step of the segmentation process of new data, fitting the model to the current can provide anatomical information to the algorithms for segmentation

1.4.4 Image Guided Surgery

Image guided surgery is another application where segmentation is useful. In order to remove lungs nodule or to do difficult biopsies, surgeons must follow complex trajectories to avoid anatomical hazards such as blood vessels or functional lungs areas.

Before surgery, visualization is done using preoperative CT scans along with three dimensional surface models of the lungs anatomy. During this procedure, the results of the preoperative segmentation may still be used. The surgeon has access to the pre-operative planning information as three dimensional models and data can be displayed in the operating room before operation.

1.4.5 Change Measurement

Using segmented lungs change in lungs can be measured. When studying chest images acquired overtime, segmenting lungs is crucial for quantitative comparisons. To this end, automatic segmentation is used to identify pathologies, which appear as bright regions in CT scans of the lungs usually. The volume of such pathologies, as measured from segmented lungs, is used to correlate with clinical changes inability and cognition.

1.4.6 Lungs Cancer Detection

Lungs cancer is the leading cause of deaths in the world. Early detection can save human life. Accordingly early detection and treatment of the lungs cancer is essential. Radiographic support for lungs cancer detection has been playing its role for the last century. CT scan is the latest modality in radiographic support. CT scan carries huge amount of data, so it is almost impossible to diagnose this huge data by human accurately. Hence computer support has become necessary. Now a days computer aided diagnose systems are in experimental phase in advance countries. For designing, developing and success of these systems, lungs segmentation is the necessary first step.

From segmented lungs, cancer detection is comparatively better judged. Both isolated and attached nodule can be detected and differentiated. Moreover, lungs cancer nodule size can also be measured from segmented lungs.

In lung cancer screening program where very huge amount of data is to be observed, lungs segmentation and then computer aided cancer detection is absolutely necessary. It manages a lot of work load.

1.5 Problems

Two fundamental facets of medical imaging make lungs segmentation a difficult problem. The First problem is due to the imaging process. The imaging process of CT is chosen such that its interactions with the lungs will provide clinically relevant information about the tissue in the resulting output image. However, it never means that the anatomical feature of lungs will be particularly separable from its surroundings. It will not be a constant grayscale value, and strong edges may not be present around its borders. In fact, the interaction of the imaging process with the lungs will often produce a “grainy” region that is more detectable by the human eye than by even sophisticated computer algorithms. This is perhaps due to noise in the imaging process as well as to non-homogeneity of the lungs itself. As such, simple image processing, such as edge detection, is not generally successful when applied to lugs segmentation.

The second problem is with the structure of the lungs itself, the complexity and variability of the lungs. Different structures of the lungs are overlapping over one another. It could not be possible to locate certain structures without detailed anatomical knowledge. Computers do not possess the expert knowledge of a radiologist, usually. This makes lungs segmentation a difficult problem, as the knowledge must either be stored into the system or provided by a human operator or an alternative method is a must.

1.6 Background

Many researchers have made efforts in the field of segmentation of the lungs from CT images and used these segmented lungs images for diagnostic purposes. However, discipline is not yet matured and efforts are on to make more achievements. Some of the related work is summarized below.

Brown et al [8] proposed knowledge based automatic method for segmentation of chest CT images. In their effort, automatic knowledge was stored in a semantic network. This knowledge was used to guide image processing routines. Instead of manual intervention, Brown et al utilized dynamic programming for searching the junction lines automatically.

Hu et al [9] presented an automatic method for lungs segmentation from CT images. The method consists of three main steps. In the first step lungs are extracted by gray level thresholding. In the second step left and right lung are separated by detecting anterior and posterior junctions. In the last step lungs boundary along with the mediastinum is refined.

W. Li et al [10] presented a fast automatic method for segmentation of lungs in CT images. The method consists of background pre processing and getting a binary image by thresholding. Then, the segmentation process was completed using mathematical morphology.

Pu et al [11] proposed Adoptive Border Marching (ABM) algorithm for lung segmentation and correction of segmentation defects caused by juxtapleural nodule while minimizing the over segmentation and under segmentation relative to the true lung border. Algorithm is automatic. The distinguishing characteristic of the algorithm is robustly including the volume of juxtapleural nodules of the lungs.

Itai et al [12] proposed a method in which initial contour points are automatically given for active contour processing by global segmentation based on threshold CT values. Then dilation is done and thus lungs are segmented.

Li and Reinhardt [13] composed three dimensional model which provided in approximate segmentation of lungs. Refinements were made by snakes to capture fine details.

Rule base techniques [14] [15] [16] [17] [18] [19] were used frequently by the researcher. In these techniques volume is found by region growing from the trachea or by using gray level threshold. After knowing approximate volume of the lungs along with airways volume, the next step is separation of left and right lung and removal of trachea and bronchi's.

Sluimer et al [20] proposed a refined segmentation-by-registration scheme in which an atlas based segmentation of the pathological lungs is refined by applying pixel classification to the border volume of the transformed probabilistic atlas. It is shown that this refinement step introduces a significant improvement in segmentation accuracy compared to a standard segmentation-by-registration approach.

Gao et al [21] described a fully automatic method for identifying the lungs in CT images. The method has three main steps. In the first step, the large airway was removed from lung region by 3D region-growth algorithm and anisotropic diffusion to smooth edges. In the second step, optimal threshold was used to automatically choose a threshold value and left and right lungs were separated by detecting the anterior and posterior junctions. Finally, lung boundary along the mediastinum was smoothed with rolling-ball algorithm.

Method of Campilho et la [22] consists an initial step to segment the patient from the background of the image, an extraction step to identify the large airways and decompose the lung parenchyma, and a final segmentation step to extract the lung region.

1.7 Proposed Method

The method is automated, optimal and adaptive. CT slices have been used as input. In the first step, gray level threshold value has been calculated. Then, the binary mask for lungs has been developed by thresholding and mathematical morphology. Finally, lungs, the ROI have been segmented from the original CT images by using binary mask.

One of the aims of the algorithm is to reduce the time needed to segment the lungs from CT slices while increasing the accuracy of the segmentation. The algorithm has been implemented in MATLAB.

1.8 Organization

Chapter 2 discusses lungs structure, lungs CT, lungs CT slices, views of the lungs CT images, and problem formulation. Chapter 3 surveys contemporary segmentation techniques for image segmentation. Chapter 4 describes proposed method and necessary implementation detail. Chapter 5 illustrates evaluation criteria, experimentations, testing, comparison and results. Chapter 6 describes conclusion and future work.

1.9 Summary

Overview of the thesis has been presented in this chapter. Objectives of the thesis have been enumerated. Important applications of the segmented lungs have been mentioned. Problems in lungs segmentation have been stated. Related literature review has been surveyed. Proposed Method in the thesis for lungs segmentation has been concisely described. At the end of the chapter organization of the thesis has been stated.

Chapter 2

Background

2.1 Introduction

This chapter describes lungs and their structure. It also explains important parts of the lungs including trachea, bronchi, bronchioles and alveoli. Then, it explains computer tomography, slices and slice thickness. At the end of the chapter, problem formulation has been described.

2.2 Lungs

The masses of alveoli constitute lungs [23] and their lobes. The lungs, liver and the heart are protected in the chest box. The chest box is formed on sides and in the front by the ribs and the intercostals muscles, and by a dumb shaped muscular diaphragm on its posterior. The lungs are enclosed in a double layered membrane called pleural membrane. There is a thin film of fluid in between the two layers. This watery fluid makes the movements of the lungs i.e. expansion & contraction easy.

2.2.1 Trachea

The air tube which is known as trachea is about 12 cm long cylindrical tube which lies in front of the esophagus. There are incomplete shaped cartilaginous rings which are regularly placed in its wall and all along its length. These rings prevent the collapsing of the tube and thus keep the air passage wide open all the time. Trachea is also lined with ciliated mucous epithelium. Any foreign particles present in the entering air gate trapped in the mucous which is moved out of the trachea by beating of the cilia in the upward direction.

2.2.2 Bronchi

The trachea on entering the chest divides into two smaller tubes which are called bronchi (single bronchus) which are similar in structure to the trachea but are smaller in diameter. They have their walls and have small irregular cartilaginous plates. Each bronchus enters into the lungs of its own side. The right bronchus branches into three and the left bronchus divides into two secondary bronchi's which serve the 3 right and 2 left lobes of the lungs respectively.

2.2.3 Bronchioles

The secondary bronchi divide into smaller and smaller branches until they end in thousands of passage ways called respiratory bronchioles. The bronchioles have not cartilaginous plates in their walls.

2.2.4 Alveoli

The walls of the respiratory bronchioles have clusters of tiny branches (like benches of grapes) that along with the respiratory bronchioles are the sites of gaseous exchange, these pouches or air sacs are called alveoli (single alveolus). The alveoli are enormous in number. Every lung has about three hundred million alveoli.

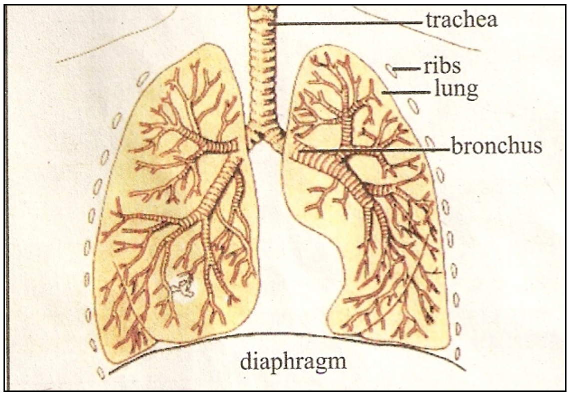

Figure 1 Labeled Lung Image

Figure 2 Labeled Lung CT Slice Image

2.3 Computer Tomography

X-Ray suffers from three limitations. Firstly, it shows two dimensional views. Accordingly, deep objects along third dimension cause confusion as the objects are superimposed upon each other. Secondly, X-Ray mainly distinguishes between boon and air in the lungs, so soft tissues and other objects can not be distinguished. These objects are only artifacts like shadow on radiographs. Thirdly, in X-Ray, it is impossible to measure the attenuation through a substance accurately. In fact it is the mean absorption by various substance through which X–Ray penetrates.

Computer Tomography (CT) surpasses all these limitations and presents a better picture of the lungs along with various tissues residing on the lungs. It measures the attenuation of the beam penetrating through the sections of the body from hundred of angles and than from these measurements, picture of interior of the body is constructed. Picture is generated through separate examinations of various contiguous cross sections seeming that body is being seen separated into different series of slices.

According to another definition, CT is a medical imaging method in which a three-dimensional image of a body structure is generated from a series of two-dimensional X-ray images taken around an axis.

In CT scanner a slice of tissue is irradiated from multiple different angles. From the opposite side, output is measured. Different tissues have different densities and attenuate the X-Ray in various proportions, denser the tissues, the lower the X- Ray beam output and vice versa. Multiple measurements from slice are noted. Then using Fast Fourier Transformation a map of various density tissues is produced.

This produced data is than converted into image which is analyzed by radiologists. Today various types of scanners exist. Depending upon the scanner types up to 4000 and even above attenuation levels may be demonstrated. The computer used for construction of image arbitrarily assigns a value to different tissues. These values are known as Hounsfield scale or Hounsfield units (HU). Usually the HU [24] for air, fat, water, soft tissues, acute blood and bone are -1000, -100, 0, 40, 60, and 2000 respectively.

Now the stage is set to generate the image. Computer assigns grey levels to different Hounsfield Unit. It is the limitation of human eye that it differentiates only 11 different shades of grey. This limitation reduced the view of image. To take advantage of huge amount of data, different windows are used. In abdominal CT Scan soft tissue of abdomen are very crucial structures, accordingly 20 grey value is assigned and window is restricted to 200. It means structures less than -80 are shown as black and structures showing 120 and above are white.

The CT Scanners can be broadly distributed into four groups. However, this distribution is not explicit. Single slice scanners are the olden style scanner. In these scanners scanning time is very large as only a single slice is generated at a time. Multi slice scanners are the scanner having multiple detectors used and hence their scanning time is short in accordance with the higher number of detectors. Helical scanner scans like spiral type moves. X-Ray source and detectors moves around the patients and the table on which the patient is lying, moves on slowly. Thus spiral type scan is obtained. Flat scanners are the scanners in which parallel slices of the body are obtained.

Slice Thickness

Slice Thickness is very important parameter in CT imaging. In fact, it is the key of CT examination. By definition, slice thickness is the interval between two consecutive passes of the scanning beam as it spirals down the patient. Small thickness means more detailed examination and better quality reformats in three dimensional images. It seems very good that examination is detailed. However, it requires more X-Ray dose and more data to process. Both these factors are critical in nature. The quantity of dose is decided as per detail examination required. There is always a compromise. The volume of data generated may lead to its own problems of handling, storing, retrieving and processing.

As an example let an image of chest is assumed having 1.25mm slice thickness. It will generate 180 images. The images used for reformat purpose are not included. If 0.625mm slice thickness is taken then 550 images will be produced.

2.4 Problem Specification

Lungs suffer from various deadly diseases such as cancer, pneumonia and tuberculoses. Biomedical support has proved to be very effective in diagnoses of such diseases. Particularly, CT scan at lungs window is an important source for diagnose of such diseases. CT images are although much better than X-rays, however, CT scan suffers at three fronts.

Firstly, it produces a large amount of data and it is impossible to accurately read and observe each slice by human observer, the doctors and the radiologist. There are a lot of chances for missing the disease indicator on the images from such a huge amount of data.

Secondly, in CT image lungs are not clearly separable from its surroundings. There are minor structures such as bronchi's on the lungs having similar look as that of the surrounding of the lungs. Pathologies on the lungs may have similar properties to that of surrounding.

Thirdly, different structures of the lungs are overlapping on one another. Certain structures are mixed with one another. Some structures around the lungs are similar to structures on the lungs.

Accordingly, segmentation of the lungs for further computer aided processing of CT images has become unavoidable. It may prove to be more beneficial for diagnoses of lungs diseases. It is helpful for diagnoses by human and input for CADs. Present research is a step up toward achieving this input for the CADs. Segmented lungs will be used for lungs cancer nodule detection and size measurement.

2.5 Summary

Lungs, computer tomography, computer aided diagnoses and problem formulation have been illustrated in this chapter. Lungs are constituted from masses of alveoli - the tiny sacs at the end of the Bronchioles. Bronchioles are the smaller airways spread from Bronchi- the large airway. CT is a worthy technique for diagnostic of lungs diseases. CT scan consists of image slices and it gives pictures of internal structure of the lungs. CT scans comprise of a large amount of data.

Chapter 3

Segmentation Overview

3.1 Introduction

Segmentation is the process of finding meaningful objects in an image. In the thesis meaningful objects are the lungs in CT images. A plethora of segmentation algorithms [25][26][27][28] are found in the literature. Selection of the technique for segmentation depends upon the nature of the segmentation problem. Majority of these algorithms are special to a particular problem, thus, having little significance for most of the other problems. This chapter surveys important segmentation techniques. These techniques include Edge detection techniques, morphological techniques, thresholding techniques, clustering techniques, and region growing techniques.

3.2 Threshold Techniques

Threshold techniques [27] are the simplest of the segmentation techniques. In this technique, a single value known as threshold is used to make a binary partition of pixel. All pixels with intensities greater than or equal to the calculated/assigned threshold are grouped together in a class and those with intensities lower than the threshold are grouped together in another class. Use of a single threshold thus results in binary segmented images.

This technique can be extended for multiple thresholds, where a region is defined by a lower threshold and an upper threshold. Then, each pixel of the input image belongs to one of the three regions based on its intensity. This extended technique is called multi-threshold.

This technique is very useful in getting segmentation done in images with a very good contrast between regions. This is usually used as the first step towards segmentation of an image.

The drawback of this technique is that the results are too tightly coupled with the thresholds used. A little change in the threshold values can produce a different segmented region. The thresholds are generally generated interactively by using feedback. Another drawback which is a direct consequence of the previous one is that the technique is very responsive to noise and intensity in-homogeneities. Thus, it cannot be easily applied to most of medical images.

3.2.1 Automatic Thresholding

Automatic Threshold makes segmentation more robust. In automatic thresholding, system automatically selects threshold value. For automatic thresholding some knowledge of the application concerned, objects in the image and environment is necessary to calculate the threshold. Especially knowledge about the objects is more helpful for finding threshold. Sizes of the objects on the image, Intensity properties of the objects, fraction of the image occupied by the objects & background and the number of objects & their different types, play decisive role in thresholding.

3.2.2 Valley Detection

In histogram, regions with uniform intensity correspond to strong peaks. Generally good threshold can be selected if the peaks in histogram are narrow, long, symmetric and separated by deep valley between the peaks.

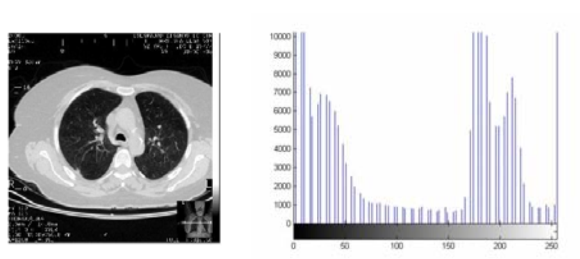

Figure 3 CT Image 1 and it's Histogram

In some cases multi-level threshold is necessary. However, it is more difficult to calculate. In such cases, more than one valley appears on the histogram of the image under observation.

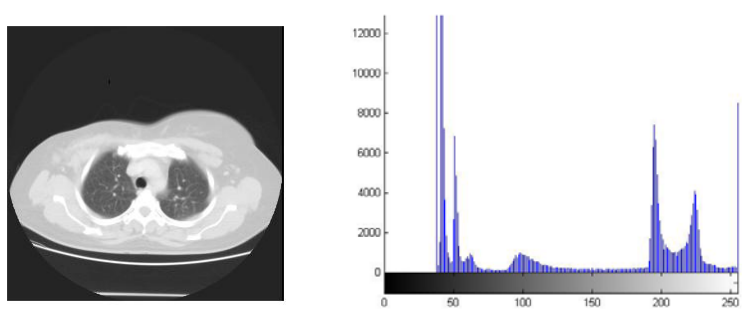

Figure 4 CT Image 2 and its Histogram

Valley detection is a simple way to find a suitable threshold. Method involves finding each of the modes (local maxima) and then finding the valley (minimum) between them. Although the method appears simple, there are two main problems with it:

- The histogram may be noisy, thus causing many local minima and maxima. To get around this, the histogram is usually smoothed before trying to find separate modes.
- The sum of two separate distributions, each with their own mode, may not produce a distribution with two distinct modes.

3.2.3 Hysteresis Thresholding

If there is clear valley in the histogram than threshold calculation is easy. Sometimes, several background pixels in the image have similar gray level value to that of background and vice versa. In such cases, there is no clear valley in the histogram of the image. Hysteresis thresholding is the technique for such a scenario. In hysteresis thresholding, two threshold values one at each side of the valley are used. Pixels above the high threshold are object pixels and pixels below the lower threshold are background pixels. Pixels between the higher and lower threshold are object pixels if and only if they are touching an object. Otherwise these pixels will be background pixels.

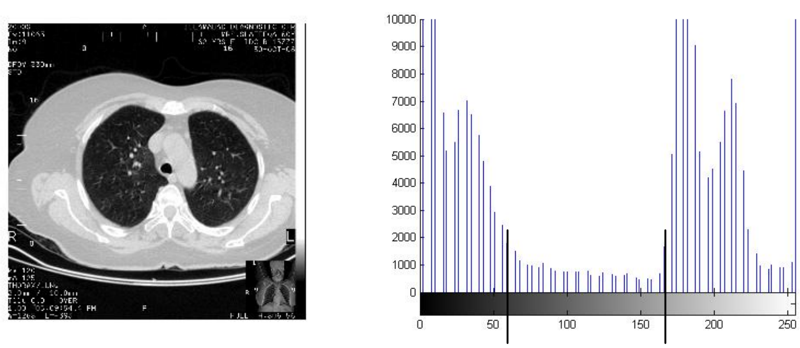

Figure 5 CT Image 3 and It's Histogram

3.2.4 P-Tile Method

This is the method requiring knowledge about the size of the object. Size may be the area or volume of the object. Let us assume that an object covers p % of the area of the image. On the histogram of the image, a curve is drawn joining top of the pixel count lines. Area under the curve is portioned into objects and background. When p % of the area is covered, threshold value is there.

3.2.5 Optimal Threshold

Assume we have an image such that it consists of two main regions. One region is object and the other is background. On threasholding, the image pixels may misclassify into object and background regions. The misclassification may be reduced if distribution of the gray levels of the pixels is already known.

If the distribution of object and background is Gaussian distribution, than probability of the pixel is given by the following formula.

$$P(z) = P(z/background)\ P(background) + P(z/object)\ P(object)$$

$$\text{Or} \quad P(z) = P_b \frac{1}{\sqrt{2\Pi\sigma_b}} e^{\frac{-(z-\mu_b)^2}{2\sigma_b^2}} + P_o \frac{1}{\sqrt{2\Pi\sigma_o}} e^{\frac{-(z-\mu_o)^2}{2\sigma_o^2}}$$

$$\text{Or} \quad P(z) = P_b p_b(z) + P_o p_o(z)$$

$p_b(z)$ is the probability distribution of the background pixels and $p_o(z)$ is the probability distribution of the pixels of object. μ_b and μ_o are means of distributions of background and object respectively. σ_b and σ_o are the standard deviations of the distributions. P_b and P_o are the Priory probabilities of the background and object pixel distributions.

Now if T is the selected threshold value, than the probability of error of classifying background pixel as object pixel is given by the following formula.

$$E_o(T) = \int_{-\infty}^{T} p_o(z)dz$$

And the probability of error of classifying a background pixel as object pixel is given by;

$$E_b(T) = \int_{T}^{\infty} p_b(z)dz$$

Total overall probability of error is as under;

$$E(T) = P_o E_o(T) + P_b E_b(T)$$

For minimize E(T),

$$\frac{dE(T)}{dT} = 0$$

The expression above is minimized when;

$$T = \frac{(\mu_b + \mu_o)}{2} + \frac{\sigma^2}{\mu_b + \mu_o} \ln(P_o/P_b) \; (\sigma_b = \sigma_o = \sigma)$$

If $P_b = P_o$ or if $\sigma = 0$, then

$$T = \frac{(\mu_b + \mu_o)}{2}$$

The procedure for selecting T is as under;

1. Histogram, h(z) of the image is found
2. Parameters μ_b, μ_o, σ_b, σ_o, P_b and P_o are selected such that

   $$P(z) = P_b p_b(z) + P_o p_o(z)$$

   Fits h(z) that is

   $$\text{Minimize Error} = \frac{1}{N} \sum_{i=1}^{N} (p(z_i) - h(z_i))^2$$

3. T is selected on the basis of formula derived above.

Optimum threshold is apparently a good method. However it suffers at two fronts. Firstly, prior probabilities usually are not known. Secondly, Objects and background distributions are not known.

3.2.6 Otsu's Method

Otsu's method [28] calculates threshold by maximizing the between class variance of object and background pixels. It assumes bimodal gray level values and does not depend on probability density function modeling.

The essence of Otsu's method is to set the threshold for object and background that can make object and background clusters as tight as possible and so minimizing overlap. Change of threshold does not affect the distribution but it essentially affects object region and background region. Change of threshold increases the spread of one region and decrease the spread of other region. Target of the threshold selection is to minimize the combined spread.

Within class variance is the weighted sum of the variances of object and background and is represented by;

$$\sigma^2_{within}(T) = n_B(T)\,\sigma^2_B(T) + n_O(T)\,\sigma^2_O(T)$$

$$n_B(T) = \sum_{i=0}^{T-1} p(i)$$

$$n_O(T) = \sum_{i=T}^{N-1} p(i)$$

$\sigma^2_B(T)$ is the variance of background pixels and $\sigma^2_O(T)$ is the variance of object pixels. [0, N-1] shows range of intensity levels.

Between classes variance is equal to the total variance of the combined distribution minus within class variance;

$$\sigma^2_{Between}(T) = \sigma^2 - \sigma^2_{Within}(T)$$

$$= n_B(T)\,[\mu_B(T) - \mu]^2 + n_O(T)\,[\mu_O(T) - \mu]^2$$

μ is the mean of whole image and σ^2 is the variance of whole image. Between classes variance is weighted variance of the cluster means themselves around the overall mean.

Putting $\mu = n_B(T)\ \mu_B(T) + n_O(T)\ \mu_O(T)$ implies that

$$\sigma^2_{Between}(T) = n_B(T)\, n_O(T)[\mu_B(T) - \mu_O(T)]$$

For each potential threshold do the following;

- Divide pixels into two groups as per threshold value.
- Calculate mean of each cluster
- Find the square of the distance between means.
- Multiply with the total pixels in one cluster times the total pixels in the other.

3.3 Edge-Detection Techniques

Edge detection techniques are the techniques which aim at detection of edges or surfaces in the images to do segmentation. Edges are found at the intersection of two regions having different intensities. Edge detection techniques work in two stages:

Edges are detected by the use of some form of differentiation. These edges are grouped together to form boundary that separate the pixels of the desired region from other region's pixels. One advantage of edge detection techniques is that they perform well on datasets having good contrast between different regions. On the down side, these algorithms sense all of the edges making it very difficult to find the region of interest and correlation between the edges. In addition, these algorithms do not function well on datasets having low contrast between the regions. These algorithms are also vulnerable to noise. Mostly, these algorithms are used coupled with other segmentation algorithms to solve a particular segmentation problem.

3.3.1 Dilation Residue Edge Detector

There are two types of residue edge detector [29] dilation residue edge detector and erosion residue edge detector. The edge of image F is E(F) and B is the structuring element. The difference set of dilation domain of F and the domain of F is known as dilation residue edge detector.

$$E(F) = (F \oplus B) - F$$

The difference set of domain of F and the erosion domain of F is known as dilation residue edge detector.

$$E(F) = F - (F \ominus B)$$

3.3.2 Sobel Edge Detector

The Sobel Edge Detector [30] consists of a pair of 3×3 convolution kernels as shown below.

-1	0	+1
-2	0	+2
-1	0	+1

+1	+2	+1
0	0	0
-1	-2	-1

One kernel is obtained by rotating the other through right angle. Kernels are used to detect edges along vertical and horizontal directions. The kernels are applied separately to the input image for producing separate measurements of the gradient component in each horizontal (*Gx*) and vertical (*Gy*) directions. Then, these horizontal and vertical gradient components are combined together to find the absolute magnitude of the gradient and the direction of the gradient at each point is found. The magnitude of the gradient is given by;

$$|G| = ((G_x)^2 + (G_y)^2)^{1/2}$$

Approximated magnitude of gradient can be calculated from the following equation;

$$|G| = | G_x | + | G_y |$$

The direction angle of the edge is given by;

$$\Theta = \arctan(G_y / G_x)$$

3.3.3 Robert Edge Detector

The Roberts Edge Detector [30] calculates a simple and quick two dimensional spatial gradient measurement of an image. Pixel values at each point in the output show the estimated magnitude of the gradient at that point.

The operator contains a pair of 2×2 convolution kernels as shown below. This operator is very close to Sobel operator.

+1	0
0	-1

Gx

0	+1
-1	0

Gy

One kernel is obtained by rotating the other through right angle. These kernels are designed to detect edges running at 45°. The kernels are applied separately to the input image for producing separate measurements of the gradient component in each horizontal (*Gx*) and vertical (*Gy*) directions. Then, these horizontal and vertical gradient components are combined together to find the absolute magnitude of the gradient and the direction of the gradient at each point is found. The magnitude of the gradient is given by;

$$|G| = ((G_x)^2 + (G_y)^2)^{1/2}$$

Approximated magnitude of gradient can be calculated from the following equation;

$$|G| = | G_x | + | G_y |$$

The direction angle of the edge is given by;

$$\Theta = \arctan(G_y / G_x) - 3\Pi/4$$

3.3.4 LOG Edge Detector

The Laplacian of Gaussian [30] is a two dimensional measure of the second spatial derivative of the image. The Laplacian highlights regions of rapid intensity change. It is therefore used for edge detection. The Laplacian operator usually takes a single gray level image as input and produces another gray level image as output. It is given by:

$$L(x,y) = \frac{\partial^2 I}{\partial x^2} + \frac{\partial^2 I}{\partial y^2}$$

L(x,y) is the Laplacian and I is the image.

We can find a convolution kernel for approximating the second derivatives in the definition of the Laplacian. The kernels are shown as under.

0	1	0
1	-4	1
0	1	0

1	1	1
1	-8	1
1	1	1

-1	2	-1
2	-4	2
-1	2	-1

These kernels are very sensitive to noise as these are approximating a second derivative measurement on the image. To counter this, the image is smoothed before applying the Laplacian filter by Gaussian smoothing.

As the convolution operation is associative, so we would convolve the Gaussian smoothing filter with the Laplacian filter first and then convolve this hybrid filter on the image to get the required result. It has the following advantages:

- The method requires far fewer arithmetic operations as both the Gaussian and the Laplacian kernels are smaller than the image.

- Only one convolution is required to be performed at run-time as the LoG kernel can be pre-calculated in advance.

The LoG centered at zero and having Gaussian standard deviation σ has the form:

$$LoG(x,y) = -\frac{1}{\pi\sigma^4}\left[1 - \frac{x^2+y^2}{2\sigma^2}\right]e^{-\frac{x^2+y^2}{2\sigma^2}}$$

3.3.5 Canny's Edge Detector

The Canny edge detector [30] is also known as the optimal edge detector. For implementing the Canny's edge detector algorithm, a series of steps are followed. The first step is to filter out noise from the original image. Gaussian filter can be calculated using a mask, and then it is used in Canny's algorithm. When the mask has been calculated, the Gaussian smoothing is performed using convolution methods. A convolution mask is usually smaller than the actual image. Resultantly, the mask is slided over the image, operating on a square of pixels at a time. The larger the width of the mask, the lower is the sensitivity to noise and vice versa. The localization error also increases slightly as the Gaussian width is increased.

After smoothing the image and eliminating the noise, the next step is to find the edge strength by taking the gradient of the image by using the Sobel Edge Detector [30]. It consists of a pair of 3×3 convolution kernels as shown below.

-1	0	+1
-2	0	+2
-1	0	+1

+1	+2	+1
0	0	0
-1	-2	-1

One kernel is obtained by rotating the other through right angle. Kernels are used to detect edges along vertical and horizontal directions. The kernels are applied separately to the input image for producing separate measurements of the gradient component in each horizontal (*Gx*) and vertical (*Gy*) directions. Then, these horizontal and vertical gradient components are combined together to find the absolute magnitude of the gradient and the direction of the gradient at each point is found. The magnitude of the gradient is given by;

$$|G| = ((G_x)^2 + (G_y)^2)^{1/2}$$

Approximated magnitude of gradient can be calculated from the following equation;

$$|G| = | G_x | + | G_y |$$

The direction angle of the edge is given by;

$$\Theta = \arctan(G_y / G_x)$$

When the edge directions are known, the next step is to relate the edge directions to a direction that is traceable in the image. If the image is of size 5x5 than pixels arrangement is as follows:

x	x	x	x	x
x	x	x	x	x
x	x	a	x	x
x	x	x	x	x
x	x	x	x	x

Consider pixel "**a**", there are only four possible directions for describing the surrounding pixels. These directions are '0 degree' in the horizontal direction, '45 degree' along the positive diagonal, '90 degree' in the vertical direction and '135 degree' along the negative diagonal. Edge orientation is required to be resolved along one of these four directions. Closest direction is given a priority. For example, if the orientation angle is 3 degree than it is made zero degree.

After resolving the edge directions, non-maximum suppression is done. Non-maximum suppression is used for suppressing any pixel value that is not considered to be an edge. Suppressing means set the equal to 0. It will provide a thin line in the output.

Finally, hysteresis is used for elimination of streaking. Streaking is the breaking up of an edge contour due to the operator output fluctuating above and below the threshold. If a single threshold, T_1, is applied to the image, and the edge having an average strength equal to T_1, then due to noise, there may be instances where the edge immersed below the threshold. Similarly, it may also pull above the threshold making an edge look like a dashed line. To avoid these problems, hysteresis is used. In hysteresis two thresholds, a high value and a low value are used. Any pixel in the image that has a value greater than T_1 is supposed to be an edge pixel, and is marked as edge. Any pixels having value less than T_2 , is also classified as non-edge pixel. Pixels having values between T_1 and T_2 may be edge pixels or non edge pixels and are connected to the edge pixel are also selected as edge pixels.

3.3.6 Morphological Gradient Edge Detector

Morphological gradient edge detector [29] is denoted by G(F). Dilation and erosion are used to compute the gradient.

$$F(F) = (F \oplus B) - (F \ominus B)$$

F is the image and B is the structuring element. The morphological gradient highlights sharp gray level transitions in the input image.

3.4 Mathematical Morphology

Mathematical morphology [31] makes use of a set of transformations for image analysis purpose. It takes out the influence of a particular shape on images via the concept of structuring elements. The Structuring Elements include the primal shape information. The shape is illustrated as a set of vectors referenced to a specific point called centre. While performing morphological operations, the centre scans the entire image and matching shape information is utilized to define the transformation. In this way, the transformed image is a function of the Structuring Element distribution on the whole image.

Morphological operations are usually simple to understand and implement. At the same time, these are usually difficult to control. For example, it is difficult to control the dilation operation unless it is given, the upper limit to the number of times of dilations. Thus, these algorithms usually require some external criteria for control. These operations also suffer from a risk of changing the morphology of the input images. It is well known that a series of dilations proceeded by erosion operations leads to loss of high frequencies and fills holes. Similarly, a series of erosions followed by dilation operations can introduce holes and high frequencies. These algorithms should not be used when accuracy is the primary concern and there is a risk of loss of important data. Morphological operations, by themselves, are not segmentation algorithms but they are usually an integral part of segmentation. Following are the important morphological operations.

3.4.1 Dilation

Dilation is a basic operation in mathematical morphology. It grows objects in a binary image. The specific manner and extent of this growing is controlled by a shape referred to as a structuring element. Centre of the structuring element is moved on each and every pixel of the target image to be dilated and growing image is found such that the image is grown up to all locations covered by structuring element. Dilation has special effect on border. When centre of the structuring element is on border pixel then about half of the structuring element would be covering the image and about half of the structuring element would be out of the boundary of the image. In dilation operation image is extended/grown up to these out side points of the structuring element.

3.4.2 Erosion

Erosion is also a basic operation in mathematical morphology. It shrinks or thins objects in a binary image. The specific manner and extent of this shrinking is controlled by a shape referred as a structuring element. Centre of the structuring element is moved on each and every pixel of the target image to be eroded and shrinked image is found such that the image is shrinked up to the locations covered by structuring element when it has its centre on the image. Erosion shrinks border. All the points of objects are excluded from object, where centre of the structuring element is on the image and even a single point of structuring element is outside the image.

3.4.3 Opening

Opening operation is derived operation in mathematical morphology. In Opening operation, image is eroded by structuring element and then result is dilated by the structuring element. It generally smoothes border of the object, breaks narrow cape and eliminates projections.

3.4.4 Closing

Closing operation is derived operation in mathematical morphology. In Closing operation image is dilated by structuring element and then result is eroded by the structuring element. It tends to smooth section of the contour. It generally fuses narrow breaks and long thin gulfs. It also eliminates small holes and fills gaps in the contour.

3.5 Clustering Techniques

Clustering techniques [26] use characteristics of the pixel and its immediate neighborhood to do clustering. Clustering can be defined as the process of grouping similar pixels into groups whose members show similar properties. Groups are the segmented regions.

Clustering-based segmentation is similar to the classifier methods but it does not use any training data. So, these techniques come under the unsupervised class of algorithms for segmentation. These algorithms cover the need for a training data by iterating between segmenting the images and typifying the properties of each class. Thus, clustering based algorithms train themselves using the available data. The various clustering algorithms on the scene today can be grouped into two broad categories:

3.5.1 Hierarchical methods

These methods consist of the techniques where the input data is not partitioned into clusters in a single step and a series of successive fusions of data are done until each cluster of size greater than one is composed of smaller clusters.

3.5.2 Non-Hierarchical methods

In Non-Hierarchical methods, the desired number of clusters is known or supposed at the beginning of the clustering process. At the end, each data pixel gets assigned to exactly one cluster in this algorithm. As in the case of classification, pixel properties (such as intensity, gradient, neighbourhood information etc.) are utilized to form an n-dimensional feature vector for each pixel. Each class of the region is supposed to form a distinct cluster in the n-dimensional feature space. A suitable clustering algorithm is then applied to each pixel in the feature space. The resulting clusters in the feature space are mapped to spatial domains to give the desired regions.

3.5.3 K-means clustering

The most commonly used clustering algorithms is K-means clustering. The input to the algorithm is a set of n-dimensional vectors having no prior knowledge about the set. Algorithm structures K (number of desired clusters in which data is to be put) disjoint nonempty subsets such that each subset minimizes some measure of dissimilarity, after processing. Thus the algorithm globally yields an optimal dissimilarity of all subsets. The dissimilarity for a pixel is its distance from the mean of each of the class. The pixel is added to the cluster whose mean is the nearest to the pixel.

3.6 Region Growing

Region growing [31] is perhaps the simplest among the hybrid techniques. Region growing is a technique to take out a connected region from an image based on some pre-defined connecting criterion. These criteria could be as simple as the pixel intensity or could be as complex as the output of any other segmentation algorithm. In the simplest form, region growing requires seed points to start with. From the seed point onward, the algorithm continues to grow till the connecting criteria is met.

3.6.1 Formulation

Let R is the whole region. Segmentation is a process portioning R into n sub-regions. These regions are R_1, R_1, R_3, R_4, ………,R_n satisfying the following conditions.

1. Union of all sub-regions is equal to whole region implying that segmentation must be complete that is every pixel must belong to some sub-region.

2. A sub-region is a connected region requiring that points in a region must be connected in some sense.

3. Intersection of two or more sub-regions is empty set indicating that regions must be disjoint.

4. $P(R_i)$ = True for i = 1, 2, 3, 4, ……………., n. $P(R_i)$ is the logical predicate defined over the the points in set R_i.

5. $P(R_i \cup R_j)$ = False for $i \neq j$, deals with the properties that must be satisfied by the pixels in a segmented region.

Like threshold, region growing is simple, but not often used for segmentation lonely. Mostly, region growing is used as a part of a segmentation technique for a particular approach. It is often used as the primary method to understand an image data before a more complex segmentation technique is applied to segment it. The primary disadvantage of this algorithm is its requirement for seed points which usually means manual interaction. Thus a seed point is needed for each region to be segmented. Region growing can also be susceptible to noise and partial images effect causing the extracted region to have holes or disconnections.

Region growing is an algorithm that groups pixels into regions on the basis of predefined criteria. Neighboring points having properties similar to that of the seeds are included in the ‘grown region’, starting with a set of seed points. These properties may be specific ranges of gray level or color etc. Selection of one or more starting points is based on the nature of the problem. When a priori information is not available, the procedure is to compute for each pixel the same set of properties that are used to assign pixels to regions during the region growing process.

The selection of homogeneity criteria depends not only on the problem under consideration, but also on the type of available image data. For example, the analysis of satellite imagery depends mostly on the use of color. In case of monochrome images, region analysis must be carried out based on gray levels and spatial properties such as texture or moments. Connectivity or adjacency information is worthy in the region-growing process. For example, visualizing a random arrangement of pixels with only three distinct gray level values and grouping pixels having same gray level to form a region without considering connectivity, would produce meaningless segmentation result.

Formulation of a stopping criterion is another problem in the region growing. Region growing must stop when no more pixels satisfy the homogeneity criteria of inclusion in that region. Criteria such as gray level, texture, and color, are local in nature and do not take part in the history of region growing. Additional criteria are required to increase the power of a region growing algorithms. These criteria utilize the concept of size, likeness between candidate pixels and the pixels grown so far. More additional criteria could be the comparison of the gray level, average gray level of the grown region and the shape of the region being grown.

3.7 Split and Merge

Split and Merge [31] technique requires the input data organized into a grid structure of regions, each region being organized into group. Any region can be split into four or eight sub regions and the appropriate four or eight regions can be merged into larger region.

Similar to region growing, the criteria for merging or growing could be simple or complex. It could be as simple as intensity value or a check or be the output of some function.

For split and merge no manual interaction is required. This is the big advantage of the algorithm over the region growing algorithm. On the down side, it needs the organized input which is usually undesirable and almost impossible for the huge datasets in use today.

Let R represent the region of entire image and P is a predicate. One approach for segmentation of R is to subdivide it successively into smaller and smaller quadrant regions so that, for segmenting R is to subdivide it successively into smaller and smaller quadrant regions so that, for any region R_i,

$$P(R_i) =\text{True}.$$

'i' denotes 1, 2, 3, ……

This approach can be implemented using quad tree. Start with the entire region, if P(R) =FALSE, we divide the input image into quadrants. If P is found false for any quadrant, we subdivide this quadrant into its own sub quadrants, and so on. The splitting technique has a suitable representation in the form of a quad tree. It is a tree in which each node has exactly four descendants. The root of the tree corresponds to the whole image and each node corresponds to subdivisions of the image.

If only splitting is utilized, the final partition may contain adjacent regions having identical properties. This drawback could be treated by allowing both merging and splitting. Two adjacent regions R_i and R_k are merged only if

$$P(R_i \cup R_k) = \text{TRUE}.$$

More variations of the basic theme of split and merge are also possible.

3.8 Summary

In this chapter an overview of the some segmentation techniques has been presented. Edge detection and morphological techniques are region based techniques. These techniques find structural properties of the region to be segmented. Structural properties such as edges are detected in the images and afterward combined to segment the region. Thresholding and clustering techniques are pixel based techniques. In these techniques segmentation decision is made on the basis of the properties of each pixel. Intensity or colour of the pixel may be considered a property. Region growing and ‘split and merge’ techniques are hybrid techniques and are combination of pixel based techniques and region based techniques. These techniques can consider both structural properties and pixel properties for segmentation.

Chapter 4

Proposed Method

4.1 Introduction

This chapter describes proposed lungs segmentation method. Threshold selection, generating binary image, removing border connected objects, filling gaps on region of interest, removing trachea and minor objects, smoothing border cavities and segmenting lungs are the steps in the method. The system takes the chest CT slice as input image. The algorithm processes it and provides segmented lungs as output. Sample input and output of the method and block diagram are shown as under:

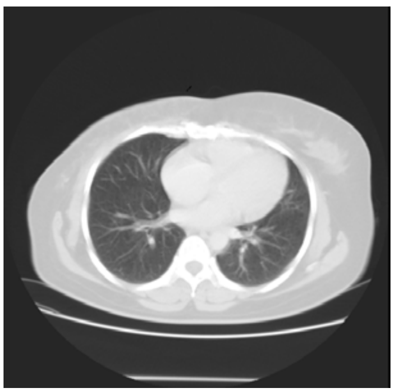

Figure 6 Sample input

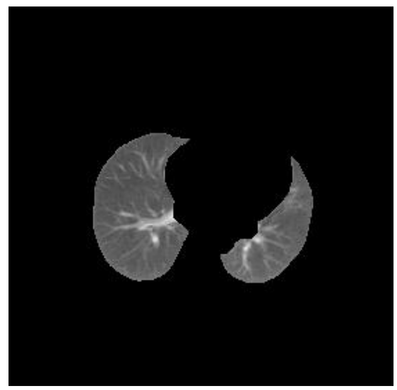

Figure 7 Sample output

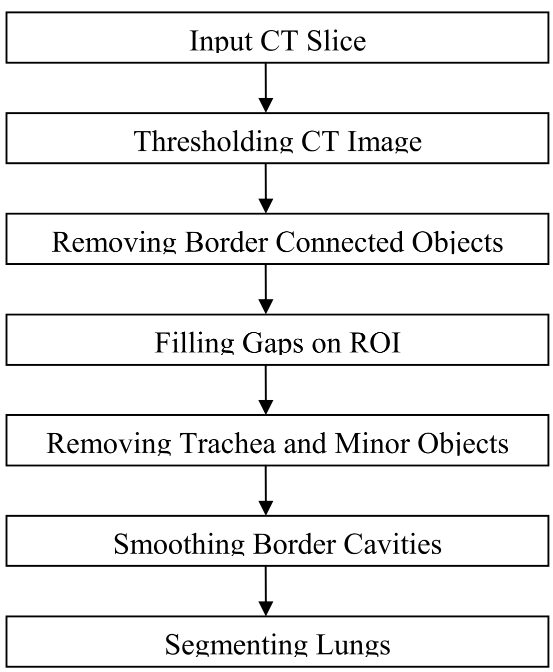

Figure 8 Block Diagram

4.2 CT Image

On visual observation, the CT image is displaying four blackish regions and one whitish region. Blackish regions are background, left lung, right lung and trachea. In some images bronchi may be there as blackish region. Whitish region is almost a ring like part surrounding and separating lungs consisting of muscle, fats etc. There is a good contrast between the blackish and whitish region on observation.

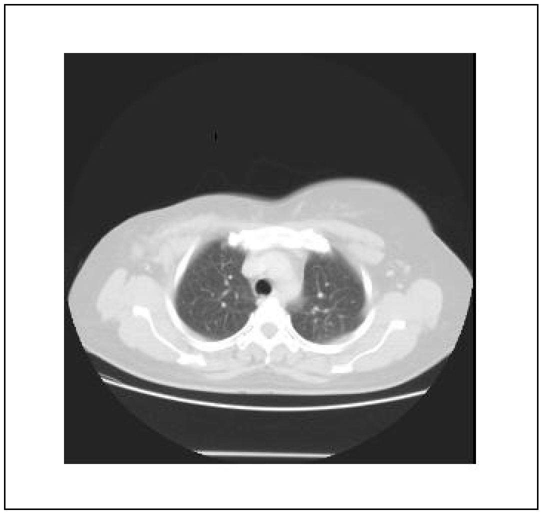

Figure 9 CT Image

Histogram of the image is a very good tool for image analysis. It is the number of pixels shown vertically associated with some frequency shown horizontally. It gives the approximated number of objects in the image. Histogram of the above CT Image is shown as under;

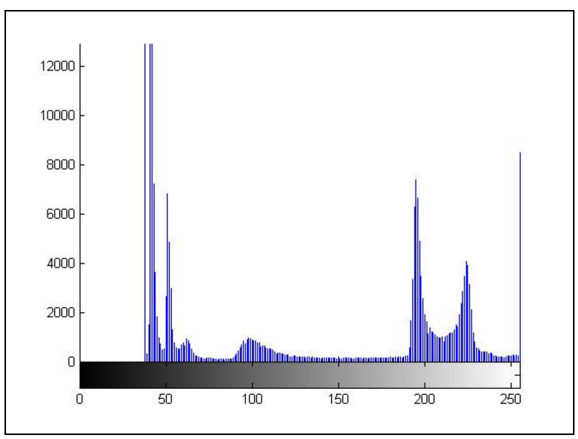

Figure 10 Histogram of CT Image

For observing hidden objects from the image, It can be equalized. Equalized image is the image having equalized histogram. In some cases equalized images provide good analysis as equalized images display some objects on images which are apparently not visible. The pixel values of the pixels of these objects may be around zero or 255. However, equalized CT Image may blend some objects. In equalized histogram, pixels are evenly spread over the available frequencies. The equalized CT Image is shown as below;

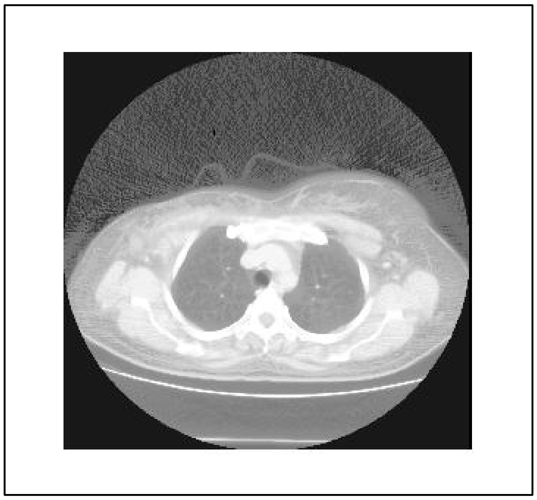

Figure 11 Equalized CT Image

Equalized CT Image has clearly shown two more objects in the CT Image. These objects are bed on which patient was lying on, while CT scan was done and a circular object around the patient caused due to penetration of X-rays through air, as air is present around the patient during scanning. Beside these two objects, some muscle and other objects have become clear. It is worth mentioning that no object has been blended in this particular image. However some objects have become blurred.

4.2 Lungs Segmentation Flow Diagram

Flow diagram of the method is shown below:

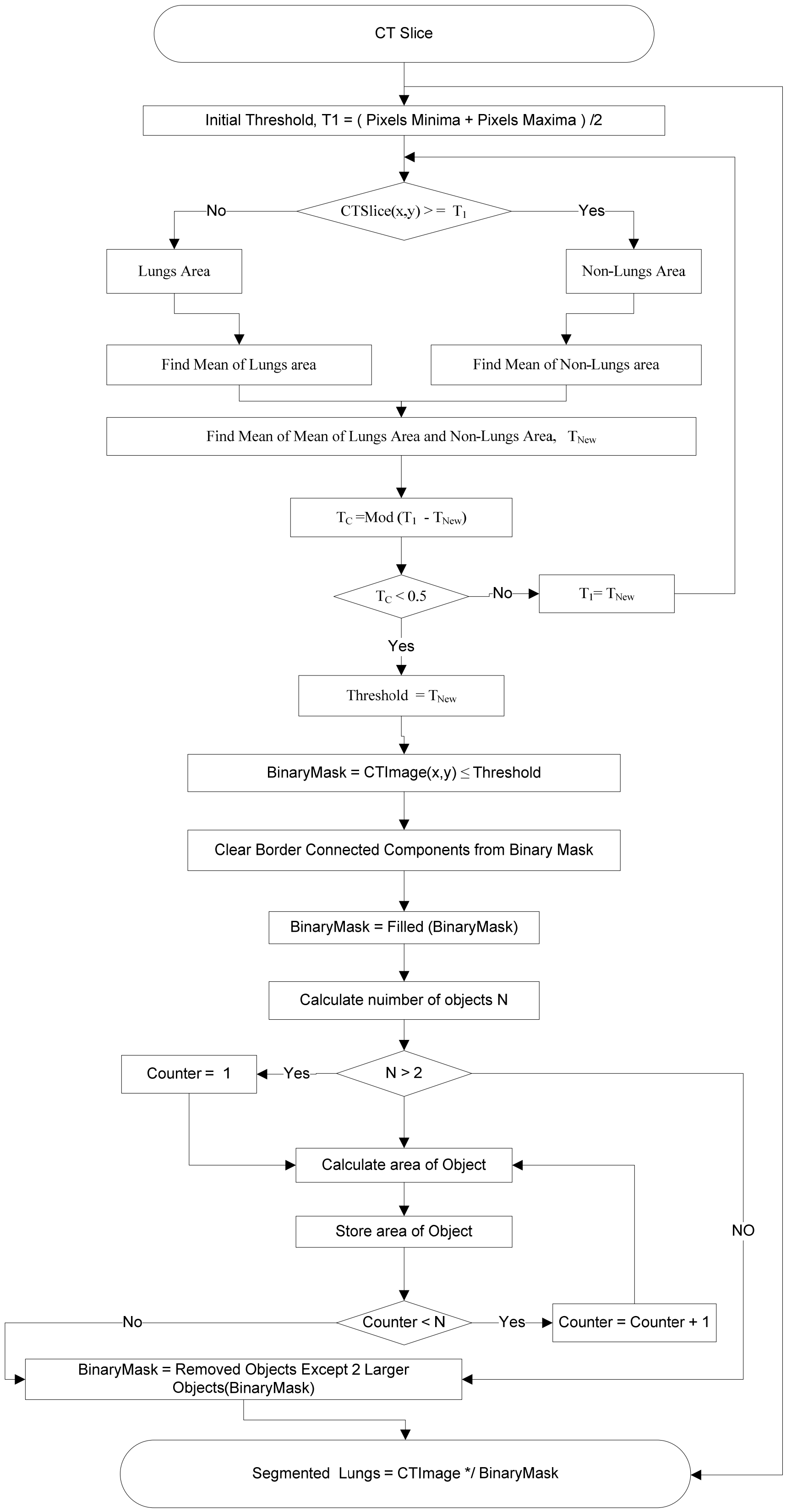

Figure 12 Flow Diagram

4.3 Threshold selection

From the input lungs slice, minimum and maximum intensity values have been calculated. These values are represented by 'Min' and 'Max'. Using these two values, initial threshold value has been calculated. Initial threshold is represented by T_1. Mathematically, T_1 is given by,

$$T_1 = (Min + Max) / 2 \quad \ldots\ldots\ldots\ldots\ldots\ldots\ldots\ldots\ldots\ldots\ldots \text{(1)}$$

The chest image is thresholded on the basis of T_1 and two pixel classes have been formed. One is approximated lungs class and the other is non-lungs class. Lungs class is represented by 'Lungs' while the non-lung class is denoted by 'NonLungs' Now, the mean value of each class is calculated. Mean value of lungs area is equal to sum of all pixels values of the lungs divided by total number of pixels of the lungs. In mathematical form,

$$\text{LungsMean} = \Sigma(\text{Values of Lungs Pixels}) / \Sigma(\text{Lungs Pixels}) \ldots\ldots\ldots\ldots\text{(2)}$$

$$\text{NonLungsMeans} = \Sigma(\text{Values of Non-Lungs pixels}) / \Sigma(\text{Non-Lungs pixels}) \ldots\text{(3)}$$

New threshold is calculated using values of LungsMean and NonLungsMeans from equation (2) and (3) above. This mean value is equal to the sum of the values of the means of the LungsMean and NonLungsMeans. New threshold is represented by T_{New}.

$$T_{New} = (\text{LungsMean} + \text{NonLungsMeans}) / 2 \quad \ldots\ldots\ldots\ldots\ldots\ldots\text{(4)}$$

A check is imposed using T_1 and T_{New} to stop the algorithm this check is given by

$$\text{Mod}\,(T_1 - T_{New}) < 0.5$$

When this check returns 'true' value than algorithm stops and T_{New} is the final threshold value. If check returns 'false' value than value of T_{New} is assigned to T_1.

This process repeats again and again till the check returns true value. Than T_{New} is the final threshold value.

Threshold value was also calculated using Otsu' s method explained in section 3.4.6. Results of both the iterative method and Otsu's method are same with difference in decimal places only. However, threshold value calculated by the iterative method was used for thresholding purpose.

4.4 Thresholding CT Image

In this step CT image has been thresholded applying calculated threshold. Gray level values of CT image having values less than or equal to threshold have been assigned value equal to 1 and gray level values of CT image having values greater than threshold have been assigned value equal to zero. That is;

$$\text{Mask}(x,y) = \begin{cases} 0 & \text{if } \text{CTImage}(x,y) > \text{Threshold} \\ 1 & \text{Otherwise} \end{cases}$$

The binary mask obtained by thresholding CT image is shown below. Black border is in fect white. It has been shown black just to visualize image size on paper.

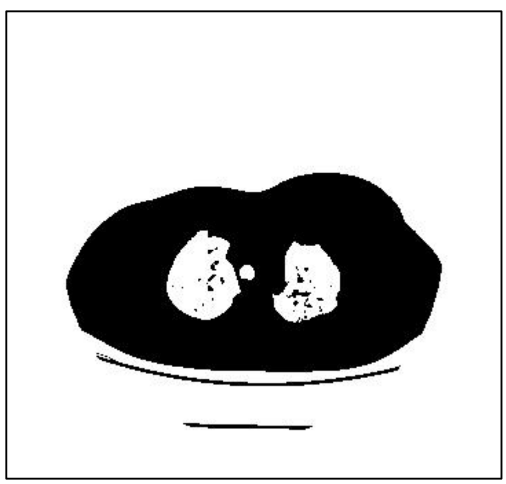

Figure 13 Thresholded CT Image

The CT image was equalized in order to get visible some hidden objects. Then equalized image was thresholded and is shown below.

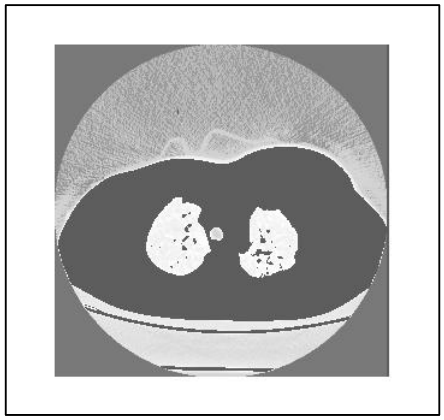

Figure 14 Equalized Histogram Thresholded CT Image

Problems

Figure 14 shows thresholded CT image. There are four obvious problems for segmenting lungs.
First, empty space around the patient in CT scan apparatus contains air. The X-ray response while passing through the air forms a circular object around the patient. Moreover patient’s built-in bed in the CT apparatus also has a different response for X-ray and forms an object. These two non-lungs objects are there in the thresholded image.

Second, some portions of lungs objects are missed. There are background like closed gaps in the left and right lungs. These gaps are due to overlapping structures of the lungs which have not been treated by the threshold method. In fact, these gaps are due to inherent problem of thresholding that it can not take locality into consideration during thresholding process. Decisions are made only on the basis of intensity / gray level value of the pixels.

Third, some lungs like objects are there beside left and right lungs. These objects have been included along lungs but actually these are not lungs portion. Usually, these objects are trachea, some vessels, minor objects introduced by the image acquiring faults in CT scanners or window size of the Hounsfield unit mapping.

Fourth, boundaries of the lungs are not smoothed. There are some gaps, cavities and bays on the boundaries of the left and right lungs. There are narrow breaks and long thin gulfs as well. This particular image has only narrow breaks on the boundary and does not have bays on it.

The solution of these problems lies in improving further the mask and then extracting the final lungs.

4.5 Removing Border Connected Objects

Thresholded CT Image specially equalized CT Image shows left and right lungs, trachea, body part surrounding lungs and empty space around the patient while CT scan is being done. It is infect background of the patient. In this step, background has been removed. All Objects of the binary image have been evaluated and object having common points with the boundary of the image have been removed, that is assigned zero value to all pixels of these objects. In equation form,

$$\text{Mask}(x,y) = \begin{cases} 0 & \text{for all pixel of Object(n) if Object(n)} \\ & \text{touches border of the Mask} \\ \text{Mask}(x,y) & \text{Otherwise} \end{cases}$$

Resultant binary mask is shown as under;

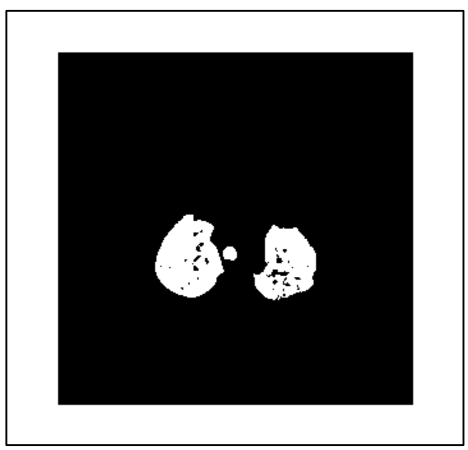

Figure 15 Background Removed Binary Mask

4.6 Filling Gaps on Region of Interest

Closed gaps on the mask are filled by an algorithm using dilation, complementation and intersection. Beginning with a point p = 1 inside the boundary, target is to fill the closed region with 1s. All non-boundary points of closed regions on the Binary

Mask are labeled as 0s. The following procedure assigns value 1 to the entire closed region within the boundary.

$$X_k = (X_{k-1} + SE) \cap (Mask)^c$$
$$K=1, 2, 3, \ldots\ldots\ldots$$

X_k is a point within the closed boundary shown on the Mask of the objects. SE is the symmetric 3 X 3 structuring element with 1 on the centre and on the 4-neighbours.

The algorithm stops at step 'k' when $X_k = X_{k-1}$. The dilation process would have filled all the area if remained unchecked. Intersection with $(Mask)^c$ at each step forces the algorithm to fill only the inside of the closed unfilled region on the Mask.

The union of the X_k and points where Mask(x,y) = 1 gives the filled binary Mask. In equation form,

$$Mask = X_k \cup (Mask(x,y) = 1)$$

Filled Binary Mask is shown in the figure below.

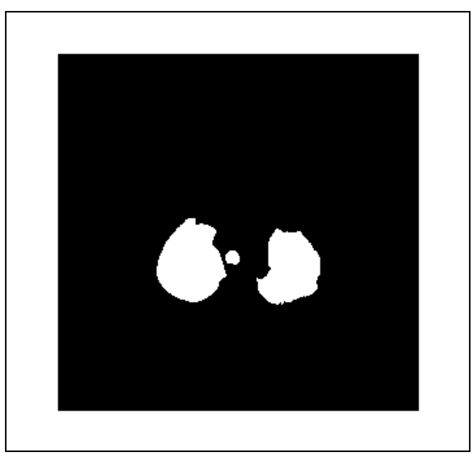

Figure 16 Filled Binary Mask

4.7 Removing Trachea and Mistaken Objects

Some component such as trachea and vessels look like lungs in the CT Slice images. Accordingly, after thresholding and filling the initial mask, some of such components are mistakenly included along the lungs. Now lungs are to be extracted from these components.

Firstly, the number of components is counted on the binary mask. If this number is less than or equal to two, then there are no additional components to remove and binary mask do not require this step. On the other hand, if the number of components/objects is greater than two then there are extra component to be removed beside left and right lungs. So further processing for removing these components is required.
Now area of each component is calculated using the following formulae.

$$\text{Area of object} = \Sigma P_i \quad \ldots\ldots\ldots\ldots\ldots\ldots\ldots\ldots\ldots\ (5)$$

Where P_i represents an arbitrary pixel and 'i' is equal to 1, 2, 3, ……………… ,n. n is the total number of pixels in the object.

Calculated area of each object has been stored in an array namely AreasObjects. A variable 'Count' is introduced for check. When area of the object is calculated, an increment is given to the 'count' (count = count + 1). The process of calculating area continues until 'count' becomes equal to the number of objects. Thus area of the all object has been calculated and stored.

Array 'AreasObjects' has been sorted in descending order. AreasObjects(0) and AreasObjects(1) are the two maximum area objects. In fact, these objects are the left lung and the right lung. Beside these two objects all objects have been removed. These are, in fact, the smaller objects mistaken for lungs. In the terminology of the image processing,

$$\text{Mask}(x,y) = \begin{cases} \text{All pixel values of AreasObjects}[i] = 0 \quad \text{if} \quad \text{AreasObject}[i] > 1, \\ \text{Mask}(x,y) \qquad \text{Otherwise} \end{cases}$$

Trachea and mistaken objects removed binary mask is shown in the figure below.

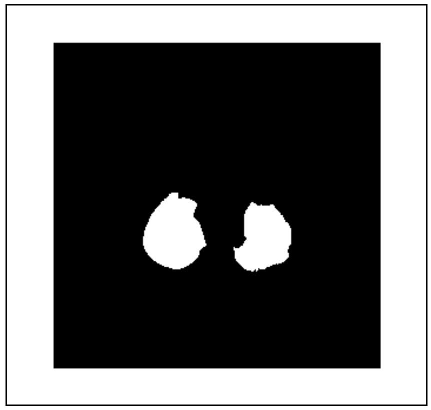

Figure 17 Trachea Removed Binary Mask

4.8 Smoothing Border Cavities

Still boundaries of the extracted lungs are not smoothed. There are some breaks and bays. Morphological closing has been used to get final lungs mask taking structuring element SE10, a disk having size equal to 10 pixels. Closing operation has bridged the bays and breaks on the border.

$$\text{Mask} = (\text{Mask} \oplus \text{SE10}) \ominus \text{SE10}$$

Final binary mask after performing close operation is shown as under;

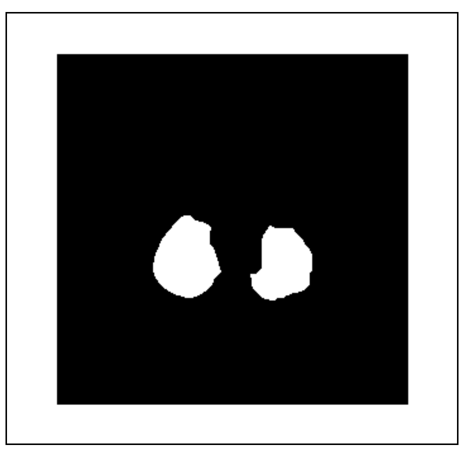

Figure 18 Final Binary Mask

4.9 Segmenting Lungs

Using the final binary mask and original image lungs has been segmented. From the original image all the pixel values have made zero where corresponding final mask values are zeros leaving all other values of the original image same. It has been done by pixel by pixel multiplication.

Segmented Lungs = Mask */ OrignalLungs

Segmented lungs are shown in the figure as under.

Figure 19 Segmented Lungs

4.10 Implementation

The method has been implemented by using Matlab, a powerful language for technical computing. Image Processing Toolbox has been used extensively in the implementation. OrigalImages, ManMarkImages are the two important folders. These folders respectively contain Original CT slice images and manually delineated lungs images delineated by a radiologist.

4.11 Summary

In this chapter, proposed method for lungs segmentation has been elaborated. Three important techniques of the image processing have been utilized in the method for lungs segmentation. These techniques are gray level thresholding, connectivity and mathematical morphology. Gray level thresholding has been used for approximating the lungs region. Connectivity has been used for removing trachea and lungs like objects. Mathematical morphology has been used for filling gaps in the lungs and smoothing boundaries of the lungs. Thus segmented lungs have been found.

Chapter 5

Results and Comparison

5.1 Introduction

This chapter describes performance metrics, dataset, experimentation, testing and comparison. Performance metrics includes precision, recall, overlapping fraction, specificity, accuracy and F-measure. Dataset consists of two complete CT Scans and 25 more CT slices. Testing describes the details of six initial experiments and results for the twenty five CT slices. Comparison section compares the results with Sluimer et al and Vinhais et al.

5.2 Performance Metrics

No standard database exists for comparing results of proposed method, as for as we know. Some researchers have tried to validate their lungs segmentation results against manually delineated lungs by radiologists. We have also adopted the same strategy. There are two classes of pixel. One is the lungs class and the other non-lungs class. Lungs class contains pixels belonging to the lungs region. The non-lungs class is the class containing pixels that are not part of the lungs. Important performance metrics for validation are:

True Positive (TP)

A pixel has been predicted as belonging to lungs region and it actually belongs to lungs region. In other words, the class of pixel has been predicted as lungs and it is the pixel belonging to lungs class.

True Negative (TN)

A pixel has been predicted as belonging to non-lungs region and it actually belongs to non-lungs region. In other words, the class of pixel has been predicted as non-lungs and it is the pixel belonging to non-lungs class.

False Negative (FN)

A pixel has been predicted as belonging to non-lungs region and it actually belongs to lungs region. In other words, the class of pixel has been predicted as non-lungs and it is the pixel belonging to lungs class.

False Positive (FP)

A pixel has been predicted as belonging to lungs region and it actually does not belong to lungs region. In other words, the class of pixel has been predicted as lungs and it is the pixel belonging to non-lungs class.

5.2.1 Overlapping Fraction

Overlapping Fraction is defined as true positives divided by sum of true positives, false negative and false positives.

$$\text{Overlapping Fraction} = TP / (TP + FN + FP)$$

5.2.2 Precision

Precision is defined as true positives divided by sum of true positives and false positives.

$$\text{Precision} = TP / (TP + FP)$$

5.2.3 Recall

Recall is defined as true positives divided by sum of true positives and false negatives. It is also known as sensitivity.

$$\text{Recall} = TP / (TP + FN)$$

5.2.4 Accuracy

Accuracy is defined as sum of true positives and true negative divided by sum of true positives, false positive, true negative and false negatives.

$$\text{Accuracy} = (TP + TN) / (TP + FP + TN + FN)$$

5.2.5 Specificity

Specificity is defined as true negative divided by sum of, true negative and false positive.

$$\text{Specificity} = (TN) / (TN + FP)$$

5.2.6 F-measure

F-measure is defined as harmonic mean of precision and recall.

$$\text{F-measure} = 2 / (1/\text{Precision}) + (1/\text{Recall})$$

5.3 Data set

Data set consists of three complete CT scans containing 20 slices each and 25 more slices thus in all 85 slices collected from NORI, Islamabad and Islamabad Diagnostic Centre, Islamabad. CT scans are in 'DICOM'(Digital Imaging and Communication in Medicine) format which is an important format in medical imaging for storage and communication purposes.

Dicom file [32] is a raw data with 'dcm' extension. It has to be processed before using. Dicom file contains header part and image data part. Header part stores information about patient, scan type, and dimension of the image etc. Usually, image data is stored as 16 bits / pixel signed value.

Randomly selected twenty five slices have been converted to bitmap (bmp) format for comparing results. Moreover, these 25 slices have also been acquired manually delineated by a radiologist.

5.4 Testing

Experiment 1

Data for the experiment consists of image1 and manually delineated image1 as shown below.

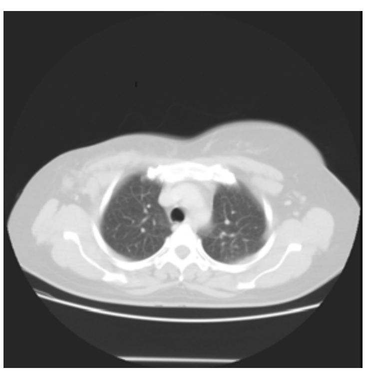

Figure 20 Original Image1

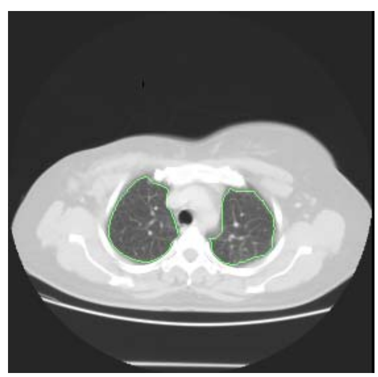

Figure 21 Manually Delineated image1

Gray level threshold value has been automatically calculated from the original image for approximating mask and found to be 129.0942. Then, the image has been thresholded on the basis of this threshold value and approximated mask has been found. Afterwards, mask have been refined by removing background, filling gaps in the mask, removing trachea, other smaller lungs like objects through an automatic process and smoothing boundaries of the mask. Finally lungs have been segmented using mask. Segmented lungs are shown as under.

Figure 22 Segmented Lungs Image1

Experiment 2

Data set for the experiment consists of image2 and manually delineated image2 as shown below.

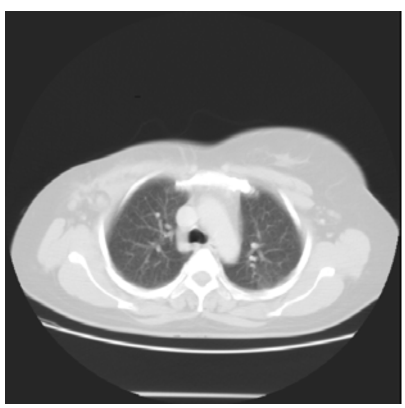

Figure 23 Original Image2

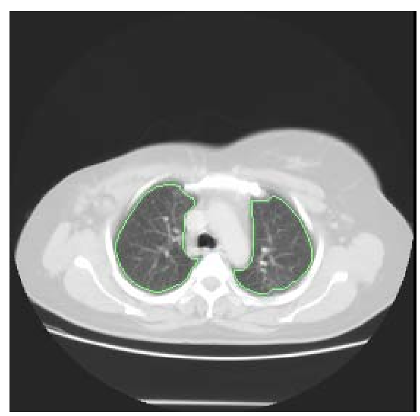

Figure 24 Manually Delineated image2

Gray level threshold value has been automatically calculated from the original image for approximating mask and found to be 128.9561. Then, the image has been thresholded on the basis of this threshold value and approximated mask has been found. Afterwards, mask have been refined by removing background, filling gaps in the mask, removing trachea, other smaller lungs like objects through an automatic process and smoothing boundaries of the mask. Finally lungs have been segmented using mask. Segmented lungs are shown as under.

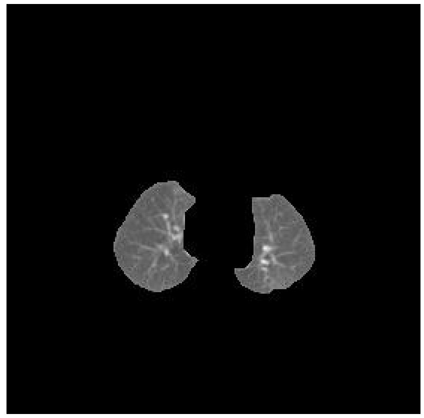

Figure 25 Segmented Lungs Image2

Experiment 3

Data set for the experiment consists of image3 and manually delineated image3 as shown below.

Figure 26 Original Image3

Figure 27 Manually Delineated image3

Gray level threshold value has been automatically calculated from the original image for approximating mask and found to be 126.7973. Then, the image has been thresholded on the basis of this threshold value and approximated mask has been found. Afterwards, mask have been refined by removing background, filling gaps in the mask, removing trachea, other smaller lungs like objects through an automatic process and smoothing boundaries of the mask. Finally lungs have been segmented using mask. Segmented lungs are shown as under.

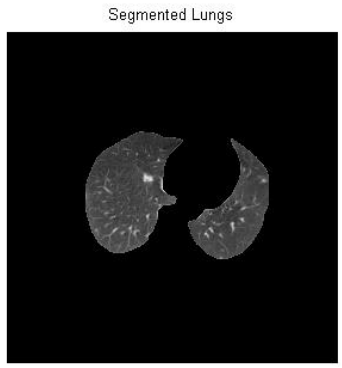

Figure 28 Segmented Lungs Image3

Experiment 4

Data set for the experiment consists of image4 and manually delineated image4 as shown below.

Figure 29 Original Image4

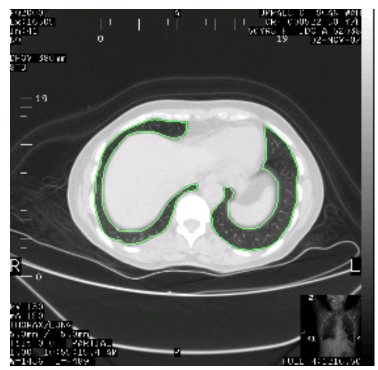

Figure 30 Manually Delineated image4

Gray level threshold value has been automatically calculated from the original image for approximating mask and found to be 127.0412. Then, the image has been thresholded on the basis of this threshold value and approximated mask has been found. Afterwards, mask have been refined by removing background, filling gaps in the mask, removing trachea, other smaller lungs like objects through an automatic process and smoothing boundaries of the mask. Finally lungs have been segmented using mask. Segmented lungs are shown as under.

Figure 31 Segmented Lungs Image4

Experiment 5

Data set for the experiment consists of image5 and manually delineated image5 as shown below.

Figure 32 Original Image5

Figure 33 Manually Delineated image5

Gray level threshold value has been automatically calculated from the original image for approximating mask and found to be 108.5809. Then, the image has been thresholded on the basis of this threshold value and approximated mask has been found. Afterwards, mask have been refined by removing background, filling gaps in the mask, removing trachea, other smaller lungs like objects through an automatic process and smoothing boundaries of the mask. Finally lungs have been segmented using mask. Segmented lungs are shown as under.

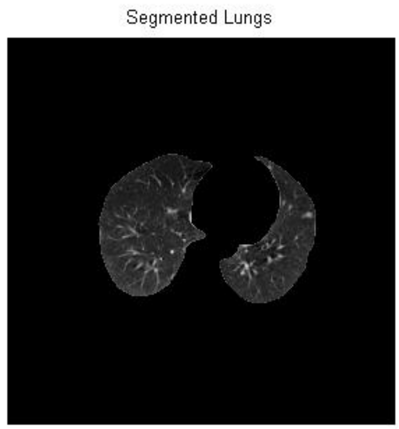

Figure 34 Segmented Lungs Image5

Experiment 6

Data set for the experiment consists of image6 and manually delineated image6 as shown below.

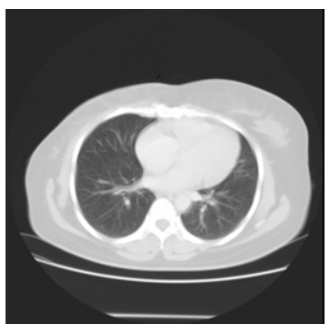

Figure 35 Original Image6

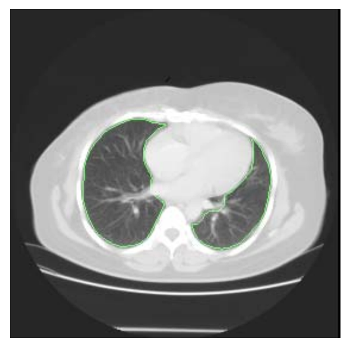

Figure 36 Manually Delineated image6

Gray level threshold value has been automatically calculated from the original image for approximating mask and found to be 131.0420. Then, the image has been thresholded on the basis of this threshold value and approximated mask has been found. Afterwards, mask have been refined by removing background, filling gaps in the mask, removing trachea, other smaller lungs like objects through an automatic process and smoothing boundaries of the mask. Finally lungs have been segmented using mask. Segmented lungs are shown as under.

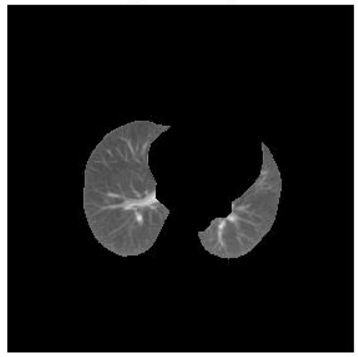

Figure 37 Segmented Lungs Image6

5.6 Results

Following table shows true positive, false negative, false positive and true negative and their means.

Table 1: Results TP FN FP and TN

Experiment	TP	FN	FP	TN
1.	4510	36	0	72182
2.	5276	35	0	71417
3.	8959	26	0	68021
4.	4065	53	0	72888
5.	9020	0	39	67947
6.	8027	43	0	68658
7.	13248	78	0	63680
8.	13579	43	0	63384
9.	12651	0	0	64355
10.	9427	0	21	67558
11.	8577	52	0	68377
12.	10138	68	0	66800
13.	1258	0	15	75733
14.	4294	50	0	72662
15.	2718	0	29	70965

Experiment	TP	FN	FP	TN
16.	3274	17	0	70421
17.	9669	0	58	63985
18.	12032	0	61	61619
19.	8137	0	60	65515
20.	1198	0	35	72479
21.	6932	0	60	66720
22.	12032	0	61	61619
23.	1434	0	7	72271
24.	11347	0	0	62365
25.	3895	39	0	69778
Means	**7428**	**22**	**18**	**68056**

Table 2 represents overlapping fraction, precision, recall, specificity, accuracy and F-measure and their means.

Table 2: Results Overlapping Fraction Precision Sensitivity, Specificity, Accuracy and F-measure

Experiment	Overlapping Fraction	Precision	Recall/ Sensitivity	Specificity	Accuracy	F-measure
1.	0.9861	1.0000	0.9921	1.0000	0.9992	0.9960
2.	0.9917	1.0000	0.9934	1.0000	0.9994	0.9967
3.	0.9959	1.0000	0.9971	1.0000	0.9995	0.9986
4.	0.9798	1.0000	0.9871	1.0000	0.9989	0.9935
5.	0.9957	0.9957	1.0000	0.9994	0.9995	0.9978
6.	0.9931	1.0000	0.9947	1.0000	0.9993	0.9973
7.	0.9917	1.0000	0.9941	1.0000	0.9986	0.9971
8.	0.9924	1.0000	0.9968	1.0000	0.9987	0.9984
9.	0.9972	1.0000	1.0000	1.0000	0.9995	1.0000
10.	0.9978	0.9978	1.0000	0.9997	0.9997	0.9989

Experiment	Overlapping Fraction	Precision	Recall/ Sensitivity	Specificity	Accuracy	F-measure
11.	0.9929	1.0000	0.9940	1.0000	0.9992	0.9970
12.	0.9925	1.0000	0.9933	1.0000	0.9990	0.9967
13.	0.9882	0.9882	1.0000	0.9998	0.9998	0.9941
14.	0.9581	1.0000	0.9885	1.0000	0.9976	0.9942
15.	0.9901	0.9934	1.0000	0.9996	0.9996	0.9947
16.	0.9950	1.0000	0.9948	1.0000	0.9997	0.9974
17.	0.9933	0.9943	1.0000	0.9991	0.9991	0.9970
18.	0.9918	0.9932	1.0000	0.9990	0.9987	0.9975
19.	0.9927	0.9927	1.0000	0.9991	0.9992	0.9963
20.	0.9716	0.9716	1.0000	0.9995	0.9995	0.9856
21.	0.9920	0.9947	1.0000	0.9991	0.9992	0.9957
22.	0.9938	0.9952	1.0000	0.9990	0.9990	0.9975
23.	0.9951	0.9951	1.0000	0.9999	0.9999	0.9976
24.	0.9992	1.0000	1.0000	1.0000	0.9999	1.0000
25.	0.9830	1.0000	0.9901	1.0000	0.9991	0.9950
Means	**0.9900**	**0.9965**	**0.9966**	**0.9997**	**0.9992**	**0.9964**

5.6 Comparison

Sluimer et al proposed segmentation by registration approach for segmenting the lungs from CT scan. They registered a scan of normal subject with abnormal subjects. They founded deformations on abnormal lung mask and refined by applying the lung mask created for normal subject and thus obtained segmentation for abnormal lungs.

Table 3: Comparison with Sluimer et al

Performance Metric	Sluimer et al [33]	Proposed Method
Accuracy	0.9500	0.9995
Sensitivity/Recall	0.9200	0.9966

Performance Metric	Sluimer et al [33]	Proposed Method
Specificity	0.9600	0.9997

Vinhais et al proposed a fully automated method for extracting the lung region from CT images based on material decomposition. They modeled the human thorax as a composition of various materials. The segmentation involves the automatic computation of threshold values. It mainly consists of patient segmentation and decomposition, large airways extraction, lung parenchyma decomposition and lung segmentation.

Table 4: Comparison with Vinhais et al

Performance Metric	Vinhais et al [22]	Proposed Method
Overlap	0.9773	0.9929
Precision	0.9882	0.9962
Sensitivity/Recall	0.9931	0.9966
F-measure	0.9885	0.9964

It is to mention that dataset for comparison of results is not the same. Vinhais et al compared the results with its own manually delineated lungs dataset. Sluimer et al compared the results with its own manually delineated lungs dataset. We compared the results with our own manually delineated lungs dataset.

5.7 Summary

Segmented lungs have been tested against manually delineated lungs on CT slices by a radiologist. Initially, six experiments had been performed. The success of these experiments paved the way for more experiments and testing. Method was applied to 3 complete CT scans comprising 20 slices each and 25 more CT slices thus in all 85 CT slices. Overlapping Fraction, Precision, Recall Accuracy, Overlapping Fraction, Specificity and F-measure have been calculated and shown in Table 2.

Chapter 6

Conclusion and Future work

Study of domain knowledge of the lungs and computer tomography of the chest was made. Different lungs diseases were studied as well. The role of CT in biomedical investigation, diagnosis and therapy of various diseases such as pneumonia, emphysema and lungs cancer was analyzed.

It has been concluded that further computer processing of the CT images is more helpful in investigation and automated diagnosis of lungs diseases such as pneumonia, tuberculoses and lungs cancer. For making more processing on CT data for diagnoses of lungs diseases, segmentation of the lungs is utmost necessary. Lungs segmentation has a lot of applications especially in computer aided diagnoses systems and visualization.

Segmentation of the lungs from each CT slices ensures that no other anatomical structure or part of the chest is on the slice except the lung. Now any conclusion made from these segmented slices makes certain that the conclusion is about the lungs only. This segmentation can be used for lungs visualization, lungs size measurement, lungs cancer detection, lungs nodule size measurement and in other similar investigations.

A novel automatic method for lungs segmentation using threshold and mathematical morphology has been proposed in the thesis. The method successfully and efficiently segments lungs from the thoracic CT slices. In the method binary mask for lungs was developed and using the binary mask, lungs has been segmented from the thoracic CT slices.

The system has been tested and compared with the manually delineated lungs on CT images by a human expert as no standard database exists for validation and comparison of the result as far as we know. The results of the system has been found very encouraging, showing mean Overlapping Fraction, mean precision, mean Sensitivity, mean Specificity, mean Accuracy and mean F-measure as 0.9900, 0.9962, 0.9966, 0.9977, 0.9992 and 0.9964 respectively.

In future, we will design and develop computer aided diagnoses system for lungs cancer detection and nodule size measurement. We shall also show the three dimensional view of the lungs from different angle on the basis of lungs segmentation presented in the thesis.

Furthermore, automatic diagnosis of tuberculosis, automatic recognition of emphysema, automatic diagnosis of pneumonia and automatic diagnoses of such other respiratory diseases will also be the target area of further research.

Moreover, we will segment other organs from chest CT including heart and liver. We shell display three dimensional view of these organs from different angles and diagnose various diseases of these segmented organs automatically.

References

[1] Edwin L. Dove, “Bio-Imaging Fundamentals”, Notes on “Computerized Tomography, Physics of Medical Imaging”, 2001
www.engineering.uiowa.edu/~bme060/Lecture/CT**Notes**.pdf

[2] Hounsfield, Godfrey N. Nobel award Address. “Computed Medical Imaging”, Medical Physics, Vol 22, 83–90, 1980

[3] M. Kausetal. “Automated Segmentation of MR Images of Brain Tumors” Academic Radiology, 218(2), 586-591, 2001

[4] C. F. Westinetal, “Tensor Controlled Local Structure Enhancement of CT Images for Bone Segmentation”, Medical Image Computing and Computer Assisted Intervention, MICCAI, 1205–1212, 1998

[5] S. Warfield et al, “Automatic Segmentation of MRI of the Knee”, ISMRM Sixth Scientific Meeting and Exhibition, April 18-24, 563, 1998

[6] T.Kapur, “Model Based Three Dimensional Medical Image Segmentation”, Ph.D. Thesis, Artificial Intelligence Laboratory, Massachusetts Institute of Technology, 1999

[7] L. M. Lorigo, O. Faugeras, W. E. L. Grimson, R. Keriven, R. Kikinis, C. F. Westin. “Geodesic Active Contours for MRI Segmentation”, International Conference on Information Processing in Medical Imaging, Vise grad, Hungary, 1999

[8] M. S. Brown, M. F. McNitt-Gray, N. J. Mankovich, J. G. Goldin, J. Hiller, L. S. Wilson, and D. R. Aberle, “Method for Segmenting Chest CT Image Data Using an Anatomical Model: Preliminary results”, IEEE Transaction on Medical Imaging, Vol. 16, 828–839, 1997

[9]Shiying Hu, Eric A. Hoffman, “Automatic Lung Segmentation for Accurate Quantitation of Volumetric X-Ray CT Images”, IEEE Transactions on Medical Imaging, Vol. 20, No. 6, 2001

[10] W. Li, S. D. Nie, J. J. Cheng, “A Fast Automatic Method of Lung Segmentation in CT Images Using Mathematical Morphology”, IFMBE Proceedings Vol. 14, Track 4, China

[11] Jiantao Pu, Justus Roos, Chin A Yi, Sandy Napel, Geoffrey D. Rubin, David S. Paik, “Adaptive Border Marching Algorithm: Automatic Lung Segmentation on Chest CT Images”, ScienceDirect, Computerized Medical Imaging and Graphics Vol. 32, 452-462, 2008

[12] Yoshinori Ital, Hyoungseop Kim, Seiji Ishikawa, “A segmentation Method of Lung Areas by Using Snakes and Automatic Detection of Abnormal Shadow on the Areas”, International Journal of Innovative Computing, Information and Control Vol. 3, No 2, 2007

[13] B. Li and J.M. Reinhardt, “Automatic Generation of 3-D Shape Models and Their Application Homographic Image Segmentation”, Proceeding SPIE (Medical Imaging), Vol. 4322, 2001.

[14] S. G. Armato and W. F. Sensakovic, “Automated Lungs Segmentation for Thoracic CT,” Academic Radiology, Vol. 11, No. 9, 1011–1021, 2004.

[15] M. S. Brown, M. F. McNitt-Gray, N. J. Mankovich, J. G. Goldin, J. Hiller, L. S. Wilson, and D. R. Aberle, “Method for Segmenting Chest CT Image Data Using an Anatomical Model: Preliminary Results,” IEEE Transaction on Medical Imaging., Vol. 16, No. 6, 828–839, 1997.

[16] S. Hu, E. A. Hoffman and J M Reinhardt, “Automatic Lungs Segmentation for Accurate Quantitaion of Volumetric X Ray CT Images”, IEEE Transaction on Medical Imaging, Vol 20, No. 6, 2001

[17] A. Silva, J. S. Silva, B. S. Santos, and C. Ferreira, “Fast Pulmonary Contour Extraction in X-ray CT Images: A Methodology and Quality Assessment,” Proceedings. SPIE, Vol. 4321, 216–224, 2001

[18] B. Zheng, J. K. Leader, G. S. Maitz, B. E. Chapman, C. R. Fuhrman, R. M. Rogers, F. C. Sciurba, A. Perez, P. Thompson, W. F. Good, and D. Gur, “A Simple Method for Automated Lung Segmentation in X-ray CT Images,” Proceedings SPIE (Medical Imaging), Vol. 5032, 1455–1463, 2003

[19] J. K. Leader, B. Zheng, R. M. Rogers, F. C. Sciurba, A. Perez, B. E. Chapman, S. Patel, C. R. Fuhrman, and D. Gur, “Automated Lung Segmentation in X-ray Computed Tomography”, Academic Radiolology, Vol. 10, No. 11, 1224–1236, 2003

[20] Ingrid Sluimer, Mathias Prokop, and Bram van Ginneken, “Toward Automated Segmentation of the Pathological Lung in CT” , IEEE Transactions on Medical Imaging, Vol. 24, No. 8, 2005

[21] Qixin Gao, ShengJun Wang, Dazhe Zhao, Jiren Liu, “Accurate Lung Segmentation For X-ray CT Images” , Third International Conference on Natural Computing (ICNC), 2007

[22] Carlos Vinhais and Aur´elio Campilho, “Lung Parenchyma Segmentation from CT Images Based on Material Decomposition”, ICIAR 2006, LNCS 4142, 624–635, 2006, Springer Verlag, Berlin, Heidelberg, 2006

[23] www.wikipedia.com/Lungs

[24] Dominic Barron, “Computer Tomography”, Department of Radiology, Leeds Teaching Hospitals St James’s University Hospital, Leeds LS9 7TF, United Kingdom, 2005

[25] R. Acharya and R. P. Menon. “A Review of Biomedical Image Segmentation Techniques”, 140–161, 1998.

[26] R. M. Haralick and L. G. Shapiro, “Image Segmentation Techniques”, Computer Vision, Graphics, and Image Processing, 29(1):100–132, Jan. 1985.

[27] N. R. Pal and S. K. Pal, “A Review on Image Segmentation Techniques”, Pattern Recognition, Vol. 26, No.9, 1277–1294, 1993.

[28] D. L. Pham, C. Xu, and J. L. Prince, “A Survey of Current Methods in Medical Image Segmentation”, Technical Report, Johns Hopkins University, Baltimore, 1998.

[29] ZahoYu-qian, Gui Wei-hua, Chen Zhen-cheng, TangJing-tian, Li Ling-yun, “Medical Images Edge detection Based on Mathematical Morphology”, Proceeding of the IEEE, Engineering in Medicine and Biology, 27th Annual Conference, Shanghai, China, 2005.

[30] http://homepages.inf.ed.ac.uk/rbf/HIPR2/sobel.htm

[31] Rafael C. Gonzalez, Richard E. Woods, “Digital Image Processing“, 2nd Edition, Pearson Education, Prentice Hall, 2002

[32] http://medical.nema.org

[33] Ingrid C. Sluimer, Meindert Neineijer, Bram Van Ginneken, “Lungs Field Segmentation from Thin-Slice CT Scans in Presence of Severe Pathology”, Proceedings of SPIE, Vol. 5370, Ballingham, WA, 2004